Relativistic distorted-wave results for nickel-like gadolinium

Peter L. Hagelstein

Physics Department, Lawrence Livermore National Laboratory, University of California, P.O. Box 808,
Livermore, California 94550

Electron collisional data are required for population kinetics modeling and spectral predictions of highly ionized ions in high-temperature plasmas. Nickel-like ions are especially interesting for their potential use in soft-x-ray laser schemes pumped by electron collisional excitation and recombination. For highly stripped ions of moderate to high Z, relativistic effects begin to play a role in the atomic-physics calculations. We have used a relativistic multiconfigurational distorted-wave model for the calculation of electron excitation cross sections and rate coefficients between the $3s^2 3p^6 3d^{10}$ Ni-like Gd ground state and the singly excited states with an N-shell electron.

I. INTRODUCTION

Nickel-like ions have been suggested as possible candidates for implementing an electron collisional excitation scheme for creating an amplifier in the extreme ultraviolet euv and soft-x-ray spectral regimes.[1,2] The nickel-like ion contains 28 electrons, and for a relatively highly stripped system, has a ground-state configuration $1s^2 2s^2 2p^6 3s^2 3p^6 3d^{10} \, ^1S_0$. This state is an analog of the $1s^2 2s^2 2p^6 \, ^1S_0$ ground state of neon-like ions, which serves as the starting point for the neon-like collisional excitation scheme.[3–15] As the neon-like system has shown significant amplification in selenium[16,17] and, since the nickel-like system is a relatively close analog, it is likely that the implementation of the collisional scheme in nickel-like ions will prove to be interesting.

We have previously analyzed the population kinetics of nickel-like europium[2] as a possible laser candidate, and found that the nickel-like Eu ion occurs under temperature and density conditions similar to that of the neon-like Se ion. In light of the successful experimental results obtained in selenium, it is compelling to keep proposed experimental conditions as near as possible to those which have been previously demonstrated, and this has guided our interest in ions in the vicinity of $_{63}$Eu and $_{64}$Gd. One advantage of the nickel-like system is that the candidate laser transition frequencies of the 4-4 transitions in Gd occur at nearly twice the frequencies of the 3-3 transitions in neon-like selenium, while the target design and input optical laser intensity is roughly the same for both systems.

We know of no previous published results for electron collisional excitation cross sections in nickel-like Gd, or any other nearby highly stripped nickel-like system. We are aware of some unpublished distorted-wave results of K. Reed in nickel-like tin which were done with the University College London code DSW,[18] and studies of M. Klapisch using his relativistic distorted-wave code.

Previous work in the area of relativistic electron collisional calculations is relatively sparse, although there are some very good works published. The first fully relativistic distorted-wave calculations of electron scattering of which we are aware was reported by Walker.[19] The close-coupling equations for electron-hydrogen scattering have been published by Carse and Walker,[20] and results for hydrogenic ions have been given by Walker.[21,22] A

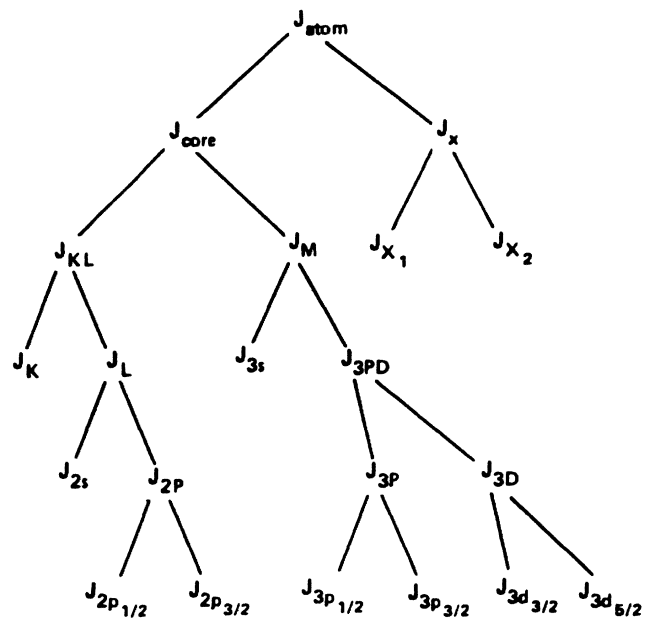

FIG. 1. Angular momentum coupling scheme used for the present set of calculations. The $1s_{1/2}$ orbital is described by J_K, and the L-shell orbitals have J values $J_{2s_{1/2}}$, $J_{2p_{1/2}}$, and $J_{2p_{3/2}}$. The two $2p$ orbitals are coupled together to form J_{2P}, which is coupled with the $2s$ orbital to form J_L. The K-shell and L-shell momenta are coupled to form an intermediate momentum J_{KL}. The M-shell orbitals with angular momenta J_{3s}, $J_{3p_{1/2}}$, $J_{3p_{3/2}}$, $J_{3d_{3/2}}$, and $J_{3d_{5/2}}$ are coupled together as shown in the figure, with intermediate momenta J_{3P}, J_{3D}, J_{3PD}, and J_M. The K-shell and L-shell coupled momentum J_{KL} is coupled with J_M to form the core momenta J_{core}. Two excited-state orbitals are included $(J_{X_1}$ and $J_{X_2})$, and are coupled to form J_X. The core electrons and the excited electrons are coupled to form the total atomic state angular momentum J_{atom}. We note that the final results obtained will be independent of angular momentum coupling scheme.

general program for calculating relativistic distorted-wave electron collisional cross sections was presented by Chang[23] and some results in Ne II were later published (Ref. 24). A very general relativistic R-matrix code has been developed by Norrington and Grant[25] which is compatible with the widely used relativistic structure code of Grant.[26-28] As this paper is being written, the general package just mentioned has not yet been released for general use among the scientific community. Relativistic distorted-wave results using an earlier version of the code described here are tabulated for a number of neon-like systems in Ref. 29. Cross sections for 2-3 excitation in the relativistic distorted-wave model have been presented for F-like selenium by Hagelstein.[30]

II. STRUCTURE CALCULATIONS

The calculations described here are based on multiconfigurational relativistic structure calculations and distorted-wave Dirac continuum states. We have employed YODA which is an atomic-physics package of Hagelstein and Jung,[31] and which calculates energy levels, oscillator strengths, photoionization cross sections, collisional cross sections, and Auger rates for a restricted angular momentum coupling scheme. YODA has been used extensively for the support of non—local-thermo-dynamic-equilibrium (NLTE) kinetics-model development at Lawrence Livermore National Laboratory for several years, and was employed in the construction of models used for the design efforts described in Rosen et al.[16]

The calculations being with spherically averaged relativistic Hartree-Fock central field orbitals which are computed using a fictitious 28-electron state which has a $1s^2 2s^2 2p^6 3s^2 3p^6 3d^9$ core and one excited electron which is distributed equally between the possible N-shells orbitals. This approach to orbital calculations is similar to methods used in the relativistic structure code (RAC) of Scofield.[32] The numerical methods used are standard and are described in a review of Grant.[33] Given the single-electron orbitals from the relativistic Hartree-Fock calculation (which are orthornormal), then a Hamiltonian is constructed assuming restricted-coupling schemes of the form shown in Fig. 1. The angular coefficients are computed using the methods of Grant and Pyper[27] and recoupling coefficients based on the algorithm of Burke.[34] Although the structure codes of Grant are general and currently widely available, at the time it seemed to be simplest to develop local tools for our specific problems. As such, these calculations are independent, and have agreed well in comparisons with other programs.

Static Coulomb terms are included in the Hamiltonian, as well as self-energy (using the hydrogenic results of Mohr[35]) and vacuum polarization (using the Uehling potential[36]). The nuclear potential is assumed to have a Fermi distribution.[37] The accuracy of the Coulomb terms in the structure calculation were verified through comparisons with codes of Pollak,[38] Scofield,[32] Desclaux,[39] and Grant[26-28] by Pollak.[40]

The Coulomb terms were evaluated through the general formulas quoted in Ref. 26 and 27,

$$\left\langle TM \left| \sum_{\substack{i,j \\ i<j}} \frac{1}{r_{ij}} \right| T'M' \right\rangle = \delta_{JJ'}\delta_{MM'} \sum_{A,B,C,D} (-1)^{\Delta}[N_A(N_B - \delta_{AB})N_C(N_D - \delta_{CD})]^{1/2}$$

$$\times \sum_{\bar{T}} (T_A\{|\bar{T}_A j_A)(T_B\{|\bar{T}_B j_B)(\bar{T}_C j_C|\}T'_C)(\bar{T}_D j_D|\}T'_D)$$

$$\times \sum_{k}\{C_d(1+\delta_{AB})^{-1}[j_A,j_D]^{-1/2}X^k(A,B,C,D)$$

$$-C_e(1-\delta_{AB})(1-\delta_{CD})[j_A,j_C]^{-1/2}X^k(A,B,D,C)\} ,$$ (2.1)

where we have followed fairly closely the notation of Grant and Pyper.[27] The number of electrons within a shell A is N_A, $(-1)^{\Delta}$ is a phase factor, and $(T_A\{|\bar{T}_A j_A)$ is a fractional parentage coefficient. The two recoupling coefficients are C_d and C_e for direct and exchange terms. The $X^k(A,B,C,D)$ functions for the Coulomb case are given by

$$X^k(A,B,C,D) = (-1)^k\langle j_A||C^{(k)}||j_c\rangle\langle j_B||C^{(k)}||j_D\rangle \Pi'(\kappa_A,\kappa_C,k)\Pi'(\kappa_B,\kappa_D,k)R^k(A,B,C,D) ,$$ (2.2)

where the $\Pi'(\kappa_A,\kappa_C,k)$ function embodies explicitly the relevant selection rules, and the radial matrix element $R^k(A,B,C,D)$ is given by

$$R^k(A,B,C,D) = \int_0^{\infty}\int_0^{\infty}[P_A(r_1)P_C(r_1)+Q_A(r_1)Q_C(r_1)]\frac{r_<^k}{r_>^{k+1}}[P_B(r_2)P_D(r_2)+Q_B(r_2)Q_D(r_2)]dr_1\,dr_2 ,$$ (2.3)

where the large components of the Dirac orbitals are denoted by $P(r)$ and the small components are denoted by $Q(r)$.

Our numerical procedures have by and large followed those described in the review paper of Grant,[33] including the use of a logarithmic grid for the computation of radial orbitals. The continuum wave functions were computed on a hybrid grid which is logarithmic near the origin and linear for large r, using techniques discussed by Hagelstein and Jung.[29]

III. COLLISION STRENGTHS AND CROSS SECTIONS

In the relativistic case, the collision strength Ω is related to the collisional cross section σ through

$$\sigma_{if}(E) = \frac{\pi a_0^2}{(2J_1+1)} \frac{1}{p^2} \Omega_{if}(E) , \qquad (3.1)$$

where the subscripts if refer to initial and final states, a_0 is the Bohr radius, $2J_i+1$ is the statistical weight of the initial state, p is the relativistic momentum in units of $1/a_0$, and E is the incident electron energy. We define further partial collision strengths Ω^J from which the total transition collision strength is computed through evaluation of the summation

$$\Omega_{if}(E) = \sum_J \Omega_{if}^J(E) , \qquad (3.2)$$

where the summation is over the total angular momentum J of the combined electron-plus-atom states which are constructed in the collisional calculations. In our definition, we have included both even and odd parities in the definition of the partial collision strength so that the sum has only a single index J. In evaluating this summation numerically, we have computed the partial collision over a predetermined range of total angular momentum J, and then used the Shank method for accelerating the summation of a series to extend the summation to large J.

The partial collision strength is defined by

$$\Omega_{if}^J(E) = \frac{1}{2} \sum_{j,j'} (2J+1) |T^J(\Gamma_i J_i j, \Gamma_f J_f j')|^2 , \qquad (3.3)$$

where $T^J(\Gamma_i J_i j, \Gamma_f J_f j')$ are the transmission matrix elements, Γ_i and Γ_f refer to suppressed quantum numbers, and j and j' refer to the continuum orbital total angular momenta. The summation is over all open channels, and in order to reduce possible confusion, these sums are over all continuum orbitals (κ would be a better index) and all possible coupling of the continuum electron to the bound-state total angular momenta which give a total J. We compute the transmission matrix elements through

$$T^J(\Gamma_i J_i j, \Gamma_f J_f j') = 4i \langle \Psi(\Gamma_i J_i j; J) | r_{12}^{-1} | \Psi(\Gamma_f J_f j'; J) \rangle . \qquad (3.4)$$

Implicit in this formula is an assumption concerning unitarity and strength of coupling. In the literature one finds expressions for the transmission matrice in terms of the reactance matrice in order to preserve unitarity (see Seaton[41] for definitions of the Born I, II, and III approximations). For highly stripped systems such as the ones under consideration here, reactance and transmission matrices tend to have magnitudes much less than unity, and the use of a simple distorted wave Born-I-type model seems appropriate.

In our model, the wave functions $\Psi(\Gamma_i J_i j; J)$ are multiconfigurational wave functions, and are expanded in terms of single configurational basis states

$$\Psi(\Gamma_i J_i j; J) = \sum_{\Gamma'} C(\Gamma_i J_i, \Gamma' J_i) \Phi(\Gamma' J_i j; J) , \qquad (3.5)$$

where $\Phi(\Gamma' J_i J)$ are single configuration states, and $C(\Gamma_i J_i, \Gamma' J_i)$ are the expansion coefficients from the bound-state structure calculations. In terms of the basis states, the transmission matrix elements are

$$T^J(\Gamma_i J_i j, \Gamma_f J_f j')$$
$$= 4i \sum_{\Gamma'} \sum_{\Gamma''} C(\Gamma_i J_i, \Gamma' J_i) C(\Gamma_f J_f, \Gamma'' J_f)$$
$$\times \langle \Phi(\Gamma' J_i j; J) | r_{12}^{-1} | \Phi(\Gamma'' J_f j'; J) \rangle . \qquad (3.6)$$

The expansion coefficients $C(\Gamma J, \Gamma' J)$ are real numbers for our problem. In the numerical calculations we have not included all terms in the sum of (3.6), as in general for a multiconfigurational problem, the majority of the terms will be quite small. We have excluded terms where the product $C(\Gamma_i J_i, \Gamma' J_i) C(\Gamma_f J_f, \Gamma'' J_f)$ is less than 0.01 in the summation in exchange for a substantial decrease in run time. This will compromise the results in cases of strongly forbidden transitions which are dominated by contributions from weak mixing between states with allowed transitions. As these transitions probably do not play much of a role in the calculation of level populations, this procedure appears to be reasonable.

There is another approximation which we have made which is worthy of some comment. All terms of Eq. (3.6) which involve matrix elements between a basis state and itself have been set to zero. The terms in question would contribute only to the elastic scattering cross sections in a single configuration approximation. When a multiconfiguration calculation is carried out, these "elastic" terms may play a role in the evaluation of the inelastic cross sections, depending on the sophistication of the approximation used. We refer interested readers to the papers by Seaton and others on the continuum Hartree-Fock equations and variational methods in collision theory.[42] The point to be made here is that the approximation used here is a quite simple (nonvariational) one, and the neglect of the elastic terms affects only a relatively minor fraction of the results quoted here (specifically transitions between states of the same total angular momentum and parity).

IV. RESULTS AND DISCUSSION

In Table I we present our results for energy-level definitions and energy levels in electron volts relative to the ground state. There are 107 states altogether, and we have attempted to group them together roughly according to configuration. The first 35 states fall cleanly in order with the N-shell splitting dominating over the $3d_{3/2}$-

TABLE I. Energy levels and state definitions for nickel-like Gd.

Level	State	J	Energy (eV)
1	$3s^2 3p_{1/2}^2 3p_{3/2}^4 3d_{3/2}^4 3d_{5/2}^6$	0	0.00
2	$3s^2 3p_{1/2}^2 3p_{3/2}^4 3d_{3/2}^4 3d_{5/2}^5 4s$	3	1028.94
3	$3s^2 3p_{1/2}^2 3p_{3/2}^4 3d_{3/2}^4 3d_{5/2}^5 4s$	2	1030.40
4	$3s^2 3p_{1/2}^2 3p_{3/2}^4 3d_{3/2}^3 3d_{5/2}^6 4s$	1	1061.98
5	$3s^2 3p_{1/2}^2 3p_{3/2}^4 3d_{3/2}^3 3d_{5/2}^6 4s$	2	1063.05
6	$3s^2 3p_{1/2}^2 3p_{3/2}^4 3d_{3/2}^4 3d_{5/2}^5 4p_{1/2}$	2	1101.06
7	$3s^2 3p_{1/2}^2 3p_{3/2}^4 3d_{3/2}^4 3d_{5/2}^5 4p_{1/2}$	3	1102.24
8	$3s^2 3p_{1/2}^2 3p_{3/2}^4 3d_{3/2}^3 3d_{5/2}^6 4p_{1/2}$	2	1134.37
9	$3s^2 3p_{1/2}^2 3p_{3/2}^4 3d_{3/2}^3 3d_{5/2}^6 4p_{1/2}$	1	1136.86
10	$3s^2 3p_{1/2}^2 3p_{3/2}^4 3d_{3/2}^4 3d_{5/2}^5 4p_{3/2}$	4	1149.36
11	$3s^2 3p_{1/2}^2 3p_{3/2}^4 3d_{3/2}^4 3d_{5/2}^5 4p_{3/2}$	2	1151.01
12	$3s^2 3p_{1/2}^2 3p_{3/2}^4 3d_{3/2}^4 3d_{5/2}^5 4p_{3/2}$	1	1151.82
13	$3s^2 3p_{1/2}^2 3p_{3/2}^4 3d_{3/2}^4 3d_{5/2}^5 4p_{3/2}$	3	1153.41
14	$3s^2 3p_{1/2}^2 3p_{3/2}^4 3d_{3/2}^3 3d_{5/2}^6 4p_{3/2}$	0	1179.48
15	$3s^2 3p_{1/2}^2 3p_{3/2}^4 3d_{3/2}^3 3d_{5/2}^6 4p_{3/2}$	1	1183.48
16	$3s^2 3p_{1/2}^2 3p_{3/2}^4 3d_{3/2}^3 3d_{5/2}^6 4p_{3/2}$	3	1183.64
17	$3s^2 3p_{1/2}^2 3p_{3/2}^4 3d_{3/2}^3 3d_{5/2}^6 4p_{3/2}$	2	1185.77
18	$3s^2 3p_{1/2}^2 3p_{3/2}^4 3d_{3/2}^4 3d_{5/2}^5 4d_{3/2}$	1	1262.13
19	$3s^2 3p_{1/2}^2 3p_{3/2}^4 3d_{3/2}^4 3d_{5/2}^5 4d_{3/2}$	4	1266.61
20	$3s^2 3p_{1/2}^2 3p_{3/2}^4 3d_{3/2}^4 3d_{5/2}^5 4d_{3/2}$	2	1267.48
21	$3s^2 3p_{1/2}^2 3p_{3/2}^4 3d_{3/2}^4 3d_{5/2}^5 4d_{3/2}$	3	1269.38
22	$3s^2 3p_{1/2}^2 3p_{3/2}^4 3d_{3/2}^4 3d_{5/2}^5 4d_{5/2}$	1	1274.65
23	$3s^2 3p_{1/2}^2 3p_{3/2}^4 3d_{3/2}^4 3d_{5/2}^5 4d_{5/2}$	5	1275.86
24	$3s^2 3p_{1/2}^2 3p_{3/2}^4 3d_{3/2}^4 3d_{5/2}^5 4d_{5/2}$	3	1278.79
25	$3s^2 3p_{1/2}^2 3p_{3/2}^4 3d_{3/2}^4 3d_{5/2}^5 4d_{5/2}$	2	1279.63
26	$3s^2 3p_{1/2}^2 3p_{3/2}^4 3d_{3/2}^4 3d_{5/2}^5 4d_{5/2}$	4	1280.32
27	$3s^2 3p_{1/2}^2 3p_{3/2}^4 3d_{3/2}^4 3d_{5/2}^5 4d_{5/2}$	0	1287.40
28	$3s^2 3p_{1/2}^2 3p_{3/2}^4 3d_{3/2}^3 3d_{5/2}^6 4d_{3/2}$	1	1298.83
29	$3s^2 3p_{1/2}^2 3p_{3/2}^4 3d_{3/2}^3 3d_{5/2}^6 4d_{3/2}$	3	1299.28
30	$3s^2 3p_{1/2}^2 3p_{3/2}^4 3d_{3/2}^3 3d_{5/2}^6 4d_{3/2}$	2	1303.71
31	$3s^2 3p_{1/2}^2 3p_{3/2}^4 3d_{3/2}^3 3d_{5/2}^6 4d_{5/2}$	1	1307.57
32	$3s^2 3p_{1/2}^2 3p_{3/2}^4 3d_{3/2}^3 3d_{5/2}^6 4d_{5/2}$	4	1310.23
33	$3s^2 3p_{1/2}^2 3p_{3/2}^4 3d_{3/2}^3 3d_{5/2}^6 4d_{5/2}$	2	1311.46
34	$3s^2 3p_{1/2}^2 3p_{3/2}^4 3d_{3/2}^3 3d_{5/2}^6 4d_{5/2}$	3	1313.02
35	$3s^2 3p_{1/2}^2 3p_{3/2}^4 3d_{3/2}^3 3d_{5/2}^6 4d_{3/2}$	0	1340.15
36	$3s^2 3p_{1/2}^2 3p_{3/2}^3 3d_{3/2}^4 3d_{5/2}^6 4s$	2	1377.90
37	$3s^2 3p_{1/2}^2 3p_{3/2}^3 3d_{3/2}^4 3d_{5/2}^6 4s$	1	1380.45
38	$3s^2 3p_{1/2}^2 3p_{3/2}^4 3d_{3/2}^4 3d_{5/2}^5 4f_{5/2}$	0	1394.07
39	$3s^2 3p_{1/2}^2 3p_{3/2}^4 3d_{3/2}^4 3d_{5/2}^5 4f_{5/2}$	1	1396.24
40	$3s^2 3p_{1/2}^2 3p_{3/2}^4 3d_{3/2}^4 3d_{5/2}^5 4f_{5/2}$	2	1399.71
41	$3s^2 3p_{1/2}^2 3p_{3/2}^4 3d_{3/2}^4 3d_{5/2}^5 4f_{5/2}$	5	1400.16
42	$3s^2 3p_{1/2}^2 3p_{3/2}^4 3d_{3/2}^4 3d_{5/2}^5 4f_{7/2}$	6	1401.32
43	$3s^2 3p_{1/2}^2 3p_{3/2}^4 3d_{3/2}^4 3d_{5/2}^5 4f_{7/2}$	2	1402.73
44	$3s^2 3p_{1/2}^2 3p_{3/2}^4 3d_{3/2}^4 3d_{5/2}^5 4f_{5/2}$	3	1402.74
45	$3s^2 3p_{1/2}^2 3p_{3/2}^4 3d_{3/2}^4 3d_{5/2}^5 4f_{5/2}$	4	1403.85
46	$3s^2 3p_{1/2}^2 3p_{3/2}^4 3d_{3/2}^4 3d_{5/2}^5 4f_{7/2}$	4	1405.54
47	$3s^2 3p_{1/2}^2 3p_{3/2}^4 3d_{3/2}^4 3d_{5/2}^5 4f_{7/2}$	5	1406.68
48	$3s^2 3p_{1/2}^2 3p_{3/2}^4 3d_{3/2}^4 3d_{5/2}^5 4f_{7/2}$	3	1407.21
49	$3s^2 3p_{1/2}^2 3p_{3/2}^4 3d_{3/2}^4 3d_{5/2}^5 4f_{7/2}$	1	1414.40

TABLE I. (Continued).

Level	State	J	Energy (eV)
50	$3s^2 3p^2_{1/2} 3p^4_{3/2} 3d^3_{3/2} 3d^6_{5/2} 4f_{7/2}$	2	1432.83
51	$3s^2 3p^2_{1/2} 3p^4_{3/2} 3d^3_{3/2} 3d^6_{5/2} 4f_{5/2}$	4	1432.96
52	$3s^2 3p^2_{1/2} 3p^4_{3/2} 3d^3_{3/2} 3d^6_{5/2} 4f_{5/2}$	2	1435.49
53	$3s^2 3p^2_{1/2} 3p^4_{3/2} 3d^3_{3/2} 3d^6_{5/2} 4f_{7/2}$	5	1436.24
54	$3s^2 3p^2_{1/2} 3p^4_{3/2} 3d^3_{3/2} 3d^6_{5/2} 4f_{5/2}$	3	1438.08
55	$3s^2 3p^2_{1/2} 3p^4_{3/2} 3d^3_{3/2} 3d^6_{5/2} 4f_{7/2}$	3	1438.84
56	$3s^2 3p^2_{1/2} 3p^4_{3/2} 3d^3_{3/2} 3d^6_{5/2} 4f_{7/2}$	4	1439.68
57	$3s^2 3p^2_{1/2} 3p^3_{3/2} 3d^4_{3/2} 3d^6_{5/2} 4p_{1/2}$	1	1450.27
58	$3s^2 3p^2_{1/2} 3p^3_{3/2} 3d^4_{3/2} 3d^6_{5/2} 4p_{1/2}$	2	1451.45
59	$3s^2 3p^2_{1/2} 3p^4_{3/2} 3d^3_{3/2} 3d^6_{5/2} 4f_{5/2}$	1	1457.66
60	$3s^2 3p^2_{1/2} 3p^3_{3/2} 3d^4_{3/2} 3d^6_{5/2} 4p_{3/2}$	3	1498.45
61	$3s^2 3p^2_{1/2} 3p^3_{3/2} 3d^4_{3/2} 3d^6_{5/2} 4p_{3/2}$	1	1498.48
62	$3s^2 3p^2_{1/2} 3p^3_{3/2} 3d^4_{3/2} 3d^6_{5/2} 4p_{3/2}$	2	1502.54
63	$3s^2 3p^2_{1/2} 3p^3_{3/2} 3d^4_{3/2} 3d^6_{5/2} 4p_{3/2}$	0	1517.64
64	$3s^2 3p_{1/2} 3p^4_{3/2} 3d^4_{3/2} 3d^6_{5/2} 4s$	0	1529.69
65	$3s^2 3p_{1/2} 3p^4_{3/2} 3d^4_{3/2} 3d^6_{5/2} 4s$	1	1531.36
66	$3s^2 3p_{1/2} 3p^4_{3/2} 3d^4_{3/2} 3d^6_{5/2} 4p_{1/2}$	1	1602.53
67	$3s^2 3p^2_{1/2} 3p^3_{3/2} 3d^4_{3/2} 3d^6_{5/2} 4d_{3/2}$	0	1611.84
68	$3s^2 3p^2_{1/2} 3p^3_{3/2} 3d^4_{3/2} 3d^6_{5/2} 4d_{3/2}$	1	1614.82
69	$3s^2 3p_{1/2} 3p^4_{3/2} 3d^4_{3/2} 3d^6_{5/2} 4p_{1/2}$	0	1615.80
70	$3s^2 3p^2_{1/2} 3p^3_{3/2} 3d^4_{3/2} 3d^6_{5/2} 4d_{3/2}$	3	1616.16
71	$3s^2 3p^2_{1/2} 3p^3_{3/2} 3d^4_{3/2} 3d^6_{5/2} 4d_{3/2}$	2	1618.39
72	$3s^2 3p^2_{1/2} 3p^3_{3/2} 3d^4_{3/2} 3d^6_{5/2} 4d_{5/2}$	4	1625.56
73	$3s^2 3p^2_{1/2} 3p^3_{3/2} 3d^4_{3/2} 3d^6_{5/2} 4d_{5/2}$	2	1626.95
74	$3s^2 3p^2_{1/2} 3p^3_{3/2} 3d^4_{3/2} 3d^6_{5/2} 4d_{5/2}$	1	1627.56
75	$3s^2 3p^2_{1/2} 3p^3_{3/2} 3d^4_{3/2} 3d^6_{5/2} 4d_{5/2}$	3	1629.57
76	$3s^2 3p_{1/2} 3p^4_{3/2} 3d^4_{3/2} 3d^6_{5/2} 4p_{3/2}$	1	1650.54
77	$3s^2 3p_{1/2} 3p^4_{3/2} 3d^4_{3/2} 3d^6_{5/2} 4p_{3/2}$	2	1652.30
78	$3s 3p^2_{1/2} 3p^4_{3/2} 3d^4_{3/2} 3d^6_{5/2} 4s$	1	1717.60
79	$3s 3p^2_{1/2} 3p^4_{3/2} 3d^4_{3/2} 3d^6_{5/2} 4s$	0	1725.83
80	$3s^2 3p^2_{1/2} 3p^3_{3/2} 3d^4_{3/2} 3d^6_{5/2} 4f_{5/2}$	1	1744.58
81	$3s^2 3p^2_{1/2} 3p^3_{3/2} 3d^4_{3/2} 3d^6_{5/2} 4f_{5/2}$	2	1747.82
82	$3s^2 3p^2_{1/2} 3p^3_{3/2} 3d^4_{3/2} 3d^6_{5/2} 4f_{5/2}$	4	1749.44
83	$3s^2 3p^2_{1/2} 3p^3_{3/2} 3d^4_{3/2} 3d^6_{5/2} 4f_{7/2}$	5	1749.92
84	$3s^2 3p^2_{1/2} 3p^3_{3/2} 3d^4_{3/2} 3d^6_{5/2} 4f_{5/2}$	3	1751.79
85	$3s^2 3p^2_{1/2} 3p^3_{3/2} 3d^4_{3/2} 3d^6_{5/2} 4f_{7/2}$	3	1753.29
86	$3s^2 3p^2_{1/2} 3p^3_{3/2} 3d^4_{3/2} 3d^6_{5/2} 4f_{7/2}$	4	1755.82
87	$3s^2 3p^2_{1/2} 3p^3_{3/2} 3d^4_{3/2} 3d^6_{5/2} 4f_{7/2}$	2	1758.80
88	$3s^2 3p_{1/2} 3p^4_{3/2} 3d^4_{3/2} 3d^6_{5/2} 4d_{3/2}$	1	1767.91
89	$3s^2 3p_{1/2} 3p^4_{3/2} 3d^4_{3/2} 3d^6_{5/2} 4d_{3/2}$	2	1768.42
90	$3s^2 3p_{1/2} 3p^4_{3/2} 3d^4_{3/2} 3d^6_{5/2} 4d_{5/2}$	2	1777.81
91	$3s^2 3p_{1/2} 3p^4_{3/2} 3d^4_{3/2} 3d^6_{5/2} 4d_{5/2}$	3	1779.45
92	$3s 3p^2_{1/2} 3p^4_{3/2} 3d^4_{3/2} 3d^6_{5/2} 4p_{1/2}$	0	1789.32
93	$3s 3p^2_{1/2} 3p^4_{3/2} 3d^4_{3/2} 3d^6_{5/2} 4p_{1/2}$	1	1792.42
94	$3s 3p^2_{1/2} 3p^4_{3/2} 3d^4_{3/2} 3d^6_{5/2} 4p_{3/2}$	2	1838.63
95	$3s 3p^2_{1/2} 3p^4_{3/2} 3d^4_{3/2} 3d^6_{5/2} 4p_{3/2}$	1	1839.97

TABLE I. (Continued).

Level	State	J	Energy (eV)
96	$3s^23p_{1/2}3p^4_{3/2}3d^4_{3/2}3d^6_{5/2}4f_{5/2}$	3	1901.83
97	$3s^23p_{1/2}3p^4_{3/2}3d^4_{3/2}3d^6_{5/2}4f_{7/2}$	3	1903.65
98	$3s^23p_{1/2}3p^4_{3/2}3d^4_{3/2}3d^6_{5/2}4f_{7/2}$	4	1905.43
99	$3s^23p_{1/2}3p^4_{3/2}3d^4_{3/2}3d^6_{5/2}4f_{5/2}$	2	1905.65
100	$3s3p^2_{1/2}3p^4_{3/2}3d^4_{3/2}3d^6_{5/2}4d_{3/2}$	1	1954.41
101	$3s3p^2_{1/2}3p^4_{3/2}3d^4_{3/2}3d^6_{5/2}4d_{3/2}$	2	1955.43
102	$3s3p^2_{1/2}3p^4_{3/2}3d^4_{3/2}3d^6_{5/2}4d_{5/2}$	3	1965.16
103	$3s3p^2_{1/2}3p^4_{3/2}3d^4_{3/2}3d^6_{5/2}4d_{5/2}$	2	1965.80
104	$3s3p^2_{1/2}3p^4_{3/2}3d^4_{3/2}3d^6_{5/2}4f_{5/2}$	2	2086.92
105	$3s3p^2_{1/2}3p^4_{3/2}3d^4_{3/2}3d^6_{5/2}4f_{5/2}$	3	2087.65
106	$3s3p^2_{1/2}3p^4_{3/2}3d^4_{3/2}3d^6_{5/2}4f_{7/2}$	4	2089.27
107	$3s3p^2_{1/2}3p^4_{3/2}3d^4_{3/2}3d^6_{5/2}4f_{7/2}$	3	2092.99

$3d_{5/2}$ splitting. The lowest states with a $3p_{3/2}$ inner-shell hole (states 36 and 37) intrude between the $4d$ and $4f$ arrays with $3d$ holes. From level 57 and above, there is considerable intermixing of configuration arrays (in terms of the order of the states).

In Table II we present wavelengths and oscillator strengths for 3-4 transitions of nickel-like Gd, and provide comparisons with experimental results of Burkhalter et al.,[43] and theoretical results of Zigler et al.[44] In general, the present results for wavelengths are in somewhat better agreement than earlier theoretical results, possibly because we may be including more states in our structure calculation (it is not immediately clear from the discussion of Ref. 44, but seems likely). The oscillator strengths are in relatively good agreement. We have also made comparisons with the RAC code of Scofield,[32] and due to the similarity in methods used obtain very nearly identical results for energy levels and oscillator strengths when the same prescription for basis radial orbitals is used.

In Table III we tabulate the cross sections in units of cm² for all transitions from the $1s^22s^22p^63s^23s^63d^{10}\,^1S_0$ ground state to all singly excited states. In Table IV we give the rate coefficients $\langle \sigma v \rangle$ which result from the cross-sectional data, tabulated in units of cm³/sec. The excitation rate coefficient is calculated assuming a nonrelativistic Maxwellian distribution

$$\langle \sigma v \rangle = \int_0^\infty \sigma(E)v(E)f(E)dE \ , \tag{4.1}$$

$$f(E)dE = \frac{2}{\pi^{1/2}} \frac{E^{1/2}}{(kT)^{3/2}} \exp\left[-\frac{E}{kT} \right] dE \ . \tag{4.2}$$

The collision strengths which can be derived from the cross-sectional data are in general well-behaved functions of energy, and for the most part conform to simple power laws. In calculating the rate coefficients, we have taken advantage of this behavior in performing a quadrature over energy numerically which is accurate for most transitions at the percent level.

TABLE II. Wavelengths and oscillator strengths for 3-4 transitions in nickel-like Gd.

Transition	Upper state	$\lambda_{\text{theor}}(\text{Å})$ (This work)	$\lambda_{\text{expt}}(\text{Å})$ Ref. 43	$\lambda_{\text{theor}}(\text{Å})$ Ref. 44	f (This work)	f Ref. 44
1-9	$3s^23p^2_{1/2}3p^4_{3/2}3d^3_{3/2}3d^6_{5/2}4p_{1/2}$	10.906	10.90	10.87	0.121	0.111
1-12	$3s^23p^2_{1/2}3p^4_{3/2}3d^4_{3/2}3d^5_{5/2}4p_{3/2}$	10.764	10.75	10.73	0.305	0.275
1-15	$3s^23p^2_{1/2}3p^4_{3/2}3d^3_{3/2}3d^6_{5/2}4p_{3/2}$	10.476	10.47	10.73	0.036	0.033
1-37	$3s^23p^2_{1/2}3p^3_{3/2}3d^4_{3/2}3d^6_{5/2}4s$	8.982	9.01	8.98	0.384	0.357
1-39	$3s^23p^2_{1/2}3p^4_{3/2}3d^4_{3/2}3d^5_{5/2}4f_{5/2}$	8.880		8.86	0.016	0.014
1-49	$3s^23p^2_{1/2}3p^4_{3/2}3d^4_{3/2}3d^5_{5/2}4f_{7/2}$	8.766	8.77	8.75	1.09	1
1-59	$3s^23p^2_{1/2}3p^4_{3/2}3d^3_{3/2}3d^6_{5/2}4f_{5/2}$	8.506	8.54	8.49	6.65	6.38
1-65	$3s^23p_{1/2}3p^4_{3/2}3d^4_{3/2}3d^6_{5/2}4s_{1/2}$	8.096			0.047	
1-68	$3s^23p^2_{1/2}3p^3_{3/2}3d^4_{3/2}3d^6_{5/2}4d_{3/2}$	7.678			0.018	
1-74	$3s^23p^2_{1/2}3p^3_{3/2}3d^4_{3/2}3d^6_{5/2}4d_{5/2}$	7.618			1.11	
1-88	$3s^23p_{1/2}3p^4_{3/2}3d^4_{3/2}3d^6_{5/2}4d_{3/2}$	7.013			0.553	
1-93	$3s3p_{1/2}3p^4_{3/2}3d^4_{3/2}3d^6_{5/2}4p_{1/2}$	6.917			0.020	
1-95	$3s3p_{1/2}3p^4_{3/2}3d^4_{3/2}3d^6_{5/2}4p_{3/2}$	6.738			0.143	

TABLE III. Electron collisional excitation cross section (cm^2) for excitation from the nickel-like ground state $3s^2 3p^2_{1/2} 3p^4_{3/2} 3d^4_{3/2} 3d^6_{5/2}$ $^1S_0$. The level energies and definitions are given in Table I.

Levels		Energy (eV) above threshold					
I	F	160.0	300.0	600.0	1000.0	1500.0	2500.0
1	2	8.521[−22]	7.031[−22]	4.874[−22]	3.227[−22]	2.088[−22]	1.032[−22]
1	3	2.332[−21]	2.127[−21]	1.809[−21]	1.527[−21]	1.294[−21]	1.011[−21]
1	4	3.721[−22]	3.068[−22]	2.119[−22]	1.394[−22]	8.969[−23]	4.404[−23]
1	5	1.699[−21]	1.542[−21]	1.300[−21]	1.086[−21]	9.126[−22]	7.054[−22]
1	6	7.935[−22]	6.746[−22]	4.911[−22]	3.360[−22]	2.214[−22]	1.092[−22]
1	7	1.334[−21]	1.171[−21]	9.234[−22]	7.142[−22]	5.545[−22]	3.839[−22]
1	8	6.277[−22]	5.234[−22]	3.692[−22]	2.451[−22]	1.576[−22]	7.603[−23]
1	9	1.964[−21]	1.923[−21]	1.833[−21]	1.757[−21]	1.677[−21]	1.537[−21]
1	10	1.099[−21]	9.189[−22]	6.519[−22]	4.358[−22]	2.823[−22]	1.378[−22]
1	11	5.886[−22]	4.998[−22]	3.630[−22]	2.469[−22]	1.612[−22]	7.821[−23]
1	12	4.060[−21]	4.064[−21]	4.011[−21]	3.969[−21]	3.898[−21]	3.679[−21]
1	13	7.542[−22]	6.662[−22]	5.305[−22]	4.136[−22]	3.232[−22]	2.258[−22]
1	14	2.139[−22]	1.842[−22]	1.369[−22]	9.552[−23]	6.395[−23]	3.219[−23]
1	15	7.409[−22]	6.947[−22]	6.165[−22]	5.509[−22]	4.979[−22]	4.319[−22]
1	16	1.111[−21]	9.840[−22]	7.878[−22]	6.182[−22]	4.855[−22]	3.405[−22]
1	17	3.733[−22]	3.142[−22]	2.245[−22]	1.505[−22]	9.684[−23]	4.601[−23]
1	18	1.641[−21]	1.385[−21]	9.911[−22]	6.695[−22]	4.375[−22]	2.175[−22]
1	19	1.669[−21]	1.421[−21]	1.043[−21]	7.381[−22]	5.194[−22]	3.107[−22]
1	20	1.582[−21]	1.363[−21]	1.024[−21]	7.470[−22]	5.445[−22]	3.450[−22]
1	21	1.138[−21]	9.465[−22]	6.562[−22]	4.260[−22]	2.657[−22]	1.215[−22]
1	22	1.023[−21]	8.571[−22]	6.064[−22]	4.027[−22]	2.577[−22]	1.238[−22]
1	23	2.124[−21]	1.765[−21]	1.231[−21]	8.051[−22]	5.075[−22]	2.380[−22]
1	24	1.367[−21]	1.138[−21]	7.952[−22]	5.205[−22]	3.276[−22]	1.527[−22]
1	25	3.133[−21]	2.907[−21]	2.534[−21]	2.190[−21]	1.895[−21]	1.522[−21]
1	26	1.056[−21]	8.852[−22]	6.283[−22]	4.247[−22]	2.830[−22]	1.542[−22]
1	27	2.899[−21]	2.656[−21]	2.248[−21]	1.863[−21]	1.534[−21]	1.132[−21]
1	28	8.950[−22]	7.521[−22]	5.336[−22]	3.561[−22]	2.285[−22]	1.099[−22]
1	29	1.205[−21]	1.005[−21]	7.040[−22]	4.631[−22]	2.930[−22]	1.378[−22]
1	30	1.923[−21]	1.779[−21]	1.545[−21]	1.330[−21]	1.147[−21]	9.207[−22]
1	31	1.084[−21]	9.126[−22]	6.516[−22]	4.366[−22]	2.828[−22]	1.381[−22]
1	32	1.533[−21]	1.304[−21]	9.564[−22]	6.732[−22]	4.706[−22]	2.778[−22]
1	33	1.601[−21]	1.407[−21]	1.108[−21]	8.550[−22]	6.641[−22]	4.649[−22]
1	34	9.926[−22]	8.251[−22]	5.737[−22]	3.718[−22]	2.314[−22]	1.051[−22]
1	35	4.496[−20]	4.161[−20]	3.598[−20]	3.038[−20]	2.545[−20]	1.917[−20]
1	36	4.613[−22]	3.958[−22]	2.911[−22]	1.991[−22]	1.298[−22]	6.281[−23]
1	37	3.025[−21]	3.041[−21]	3.092[−21]	3.108[−21]	3.103[−21]	3.054[−21]
1	38	8.880[−22]	7.429[−22]	5.227[−22]	3.459[−22]	2.210[−22]	1.054[−22]
1	39	2.475[−21]	2.098[−21]	1.527[−21]	1.065[−21]	7.371[−22]	4.280[−22]
1	40	2.579[−21]	2.143[−21]	1.487[−21]	8.679[−22]	6.074[−22]	2.814[−22]
1	41	1.493[−21]	1.228[−21]	8.682[−22]	5.918[−22]	4.057[−22]	2.416[−22]
1	42	2.504[−21]	2.036[−21]	1.391[−21]	8.883[−22]	5.455[−22]	2.443[−22]
1	43	1.496[−21]	1.211[−21]	8.216[−22]	5.204[−22]	3.161[−22]	1.389[−22]
1	44	1.783[−21]	1.449[−21]	9.902[−22]	6.360[−22]	3.956[−22]	1.857[−22]
1	45	1.370[−21]	1.103[−21]	7.397[−22]	4.622[−22]	2.768[−22]	1.190[−22]
1	46	1.729[−21]	1.399[−21]	9.741[−22]	5.989[−22]	3.637[−22]	1.601[−22]
1	47	1.005[−21]	8.042[−22]	5.361[−22]	3.374[−22]	2.094[−22]	1.052[−22]
1	48	2.871[−21]	2.647[−21]	2.308[−21]	1.994[−21]	1.723[−21]	1.374[−21]
1	49	2.275[−20]	2.186[−20]	2.029[−20]	1.870[−20]	1.728[−20]	1.508[−20]
1	50	2.490[−21]	2.047[−21]	1.429[−21]	9.362[−22]	5.903[−22]	2.757[−22]
1	51	1.522[−21]	1.239[−21]	8.476[−22]	5.417[−22]	3.325[−22]	1.487[−22]
1	52	1.339[−21]	1.089[−21]	7.445[−22]	4.755[−22]	2.914[−22]	1.297[−22]
1	53	1.252[−21]	1.030[−21]	7.274[−22]	4.955[−22]	3.398[−22]	2.034[−22]
1	54	1.094[−21]	8.884[−22]	6.073[−22]	3.902[−22]	2.433[−22]	1.157[−22]
1	55	2.528[−21]	2.306[−21]	1.977[−21]	1.680[−21]	1.433[−21]	1.127[−21]
1	56	1.132[−21]	9.101[−22]	6.089[−22]	3.788[−22]	2.254[−22]	9.551[−23]
1	57	3.657[−22]	3.036[−22]	2.158[−22]	1.455[−22]	9.591[−23]	4.926[−23]
1	58	1.575[−21]	1.480[−21]	1.329[−21]	1.183[−21]	1.051[−21]	8.713[−22]
1	59	1.216[−19]	1.177[−19]	1.107[−19]	1.029[−19]	9.578[−20]	8.445[−20]

TABLE III. (*Continued*).

| Levels | | Energy (eV) above threshold | | | | | |
I	F	160.0	300.0	600.0	1000.0	1500.0	2500.0
1	60	6.227[−22]	5.291[−22]	3.868[−22]	2.680[−22]	1.805[−22]	9.376[−22]
1	61	3.676[−22]	3.094[−22]	2.220[−22]	1.511[−22]	1.005[−22]	5.210[−23]
1	62	1.025[−21]	9.735[−22]	8.892[−22]	8.057[−22]	7.281[−22]	6.178[−22]
1	63	2.322[−20]	2.170[−20]	1.916[−20]	1.660[−20]	1.420[−20]	1.100[−20]
1	64	8.031[−23]	6.958[−23]	5.283[−23]	3.756[−23]	2.532[−23]	1.281[−23]
1	65	5.231[−22]	4.899[−22]	4.419[−22]	3.977[−22]	3.624[−22]	3.245[−22]
1	66	2.583[−22]	2.173[−22]	1.589[−22]	1.101[−22]	7.413[−23]	3.879[−23]
1	67	1.508[−22]	1.301[−22]	9.887[−23]	7.069[−23]	4.846[−23]	2.520[−23]
1	68	4.444[−22]	3.986[−22]	3.306[−22]	2.687[−22]	2.194[−22]	1.676[−22]
1	69	1.447[−20]	1.357[−20]	1.208[−20]	1.053[−20]	9.085[−21]	7.103[−21]
1	70	1.246[−21]	1.155[−21]	1.011[−21]	8.704[−22]	7.449[−22]	5.824[−22]
1	71	2.999[−22]	2.559[−22]	1.900[−22]	1.329[−22]	8.902[−23]	4.466[−23]
1	72	7.485[−22]	6.336[−22]	4.645[−22]	3.214[−22]	2.143[−22]	1.080[−22]
1	73	3.964[−22]	3.414[−22]	2.572[−22]	1.825[−22]	1.240[−22]	6.334[−23]
1	74	5.641[−21]	5.741[−21]	5.910[−21]	6.108[−21]	6.211[−21]	6.264[−21]
1	75	6.456[−22]	5.975[−22]	5.201[−22]	4.453[−22]	3.789[−22]	2.942[−22]
1	76	3.775[−22]	3.187[−22]	2.332[−22]	1.619[−22]	1.095[−22]	5.774[−23]
1	77	8.441[−22]	7.951[−22]	7.170[−22]	6.421[−22]	5.742[−22]	4.833[−22]
1	78	1.510[−22]	1.293[−22]	9.568[−23]	6.735[−23]	4.632[−23]	2.507[−23]
1	79	8.900[−21]	8.404[−21]	7.580[−21]	6.678[−21]	5.825[−21]	4.628[−21]
1	80	8.394[−22]	7.087[−22]	5.176[−22]	3.548[−22]	2.343[−22]	1.171[−22]
1	81	1.402[−21]	1.224[−21]	9.605[−22]	7.312[−22]	5.555[−22]	3.723[−22]
1	82	1.037[−21]	9.411[−22]	7.951[−22]	6.632[−22]	5.565[−22]	4.341[−22]
1	83	1.268[−21]	1.074[−21]	7.898[−22]	5.450[−22]	3.624[−22]	1.827[−22]
1	84	8.867[−22]	7.453[−22]	5.397[−22]	3.662[−22]	2.390[−22]	1.172[−22]
1	85	5.521[−22]	4.625[−22]	3.330[−22]	2.241[−22]	1.450[−22]	6.998[−23]
1	86	5.614[−22]	5.108[−22]	4.357[−22]	3.697[−22]	3.174[−22]	2.574[−22]
1	87	1.244[−20]	1.217[−20]	1.164[−20]	1.098[−20]	1.023[−20]	8.983[−21]
1	88	1.753[−21]	1.813[−21]	1.926[−21]	2.034[−21]	2.146[−21]	2.242[−21]
1	89	3.093[−22]	2.647[−22]	1.986[−22]	1.400[−22]	9.524[−23]	4.947[−23]
1	90	3.707[−22]	3.327[−22]	2.509[−22]	1.827[−22]	1.275[−22]	6.794[−23]
1	91	7.098[−22]	6.554[−22]	5.696[−22]	4.860[−22]	4.129[−22]	3.206[−22]
1	92	4.709[−23]	4.102[−23]	3.149[−23]	2.256[−23]	1.540[−23]	7.910[−24]
1	93	1.210[−22]	1.111[−22]	9.659[−23]	8.400[−23]	7.520[−23]	6.719[−23]
1	94	2.048[−22]	1.777[−22]	1.348[−22]	9.544[−23]	6.436[−23]	3.275[−23]
1	95	3.977[−22]	3.954[−22]	3.962[−22]	4.055[−22]	4.205[−22]	4.478[−22]
1	96	5.301[−22]	4.532[−22]	3.379[−22]	2.367[−22]	1.595[−22]	8.160[−23]
1	97	9.106[−22]	7.738[−22]	5.703[−22]	3.944[−22]	2.621[−22]	1.315[−22]
1	98	6.742[−22]	6.132[−22]	5.199[−22]	4.345[−22]	3.649[−22]	2.848[−22]
1	99	5.853[−21]	5.721[−21]	5.475[−21]	5.173[−21]	4.841[−21]	4.283[−21]
1	100	1.445[−22]	1.228[−22]	9.141[−23]	6.440[−23]	4.408[−23]	2.333[−23]
1	101	4.762[−22]	4.550[−22]	4.197[−22]	3.848[−22]	3.528[−22]	3.071[−22]
1	102	3.018[−22]	2.582[−22]	1.947[−22]	1.391[−22]	9.669[−23]	5.227[−23]
1	103	1.010[−21]	9.933[−22]	9.618[−22]	9.218[−22]	8.758[−22]	7.930[−22]
1	104	4.221[−22]	3.653[−22]	2.781[−22]	1.988[−22]	1.364[−22]	7.139[−23]
1	105	6.986[−22]	5.213[−22]	5.010[−22]	3.891[−22]	2.980[−22]	1.967[−22]
1	106	7.551[−22]	6.530[−22]	4.964[−22]	3.541[−22]	2.425[−22]	1.264[−22]
1	107	2.596[−21]	2.554[−21]	2.460[−21]	2.327[−21]	2.166[−21]	1.881[−21]

The strongest collisional transition between the ground state and the excited states is between level 1 and level 59 ($\sigma = 1.2 \times 10^{-19}$ cm^2 at 160 eV above threshold). The transition is a dipole-allowed $3d_{3/2}$-$4f_{5/2}$ transition with a very large oscillator strength (6.65). Other dipole-allowed transitions with large oscillator strengths have corresponding large collisional cross sections; for example, the transitions to level 49 (a $3d_{5/2}$-$4f_{7/2}$ transition) and to

level 74 (a $3p_{3/2}$-$4d_{5/2}$ transition), with cross sections of 2.3×10^{-20} cm^2 and 5.6×10^{-20} cm^2, respectively.

Transitions to $J = 0$ excited states may be large when the excited electron is of the same J and parity as the hole. There are 5 examples of this type of transition, including transition to levels 27, 35, 63, 69, and 79. Of these transitions, three are exceptionally strong transitions: 35 ($3d_{3/2}$-$4d_{3/2}$) with a cross section of 4.5×10^{-20}

TABLE IV. Rate coefficients (cm^2/sec) for excitation from the nickel-like ground state $3s^23p^2_{1/2}3p^4_{3/2}3d^4_{3/2}3d^6_{5/2}$ $^1S_0$. The excited-state level definitions and energies are given in Table I.

Levels		Electron temperature (eV)					
I	F	500.0	700.0	1000.0	1500.0	2000.0	2500.0
1	2	3.283[−13]	4.653[−13]	5.508[−13]	5.561[−13]	5.131[−13]	4.638[−13]
1	3	1.110[−12]	1.728[−12]	2.309[−12]	2.744[−12]	2.883[−12]	2.903[−12]
1	4	1.370[−13]	1.974[−13]	2.363[−13]	2.403[−13]	2.225[−13]	2.014[−13]
1	5	7.666[−13]	1.208[−12]	1.626[−12]	1.940[−12]	2.039[−12]	2.053[−12]
1	6	2.898[−13]	4.315[−13]	5.311[−13]	5.536[−13]	5.195[−13]	4.746[−13]
1	7	5.305[−13]	8.272[−13]	1.088[−12]	1.253[−12]	1.284[−12]	1.268[−12]
1	8	2.132[−13]	3.204[−13]	3.958[−13]	4.122[−13]	3.859[−13]	3.517[−13]
1	9	9.426[−13]	1.645[−12]	2.449[−12]	3.230[−12]	3.607[−12]	3.778[−12]
1	10	3.678[−13]	5.582[−13]	6.952[−13]	7.292[−13]	6.855[−13]	6.265[−13]
1	11	2.005[−13]	3.062[−13]	3.835[−13]	4.045[−13]	3.815[−13]	3.494[−13]
1	12	2.000[−12]	3.577[−12]	5.451[−12]	7.349[−12]	8.308[−12]	8.772[−12]
1	13	2.827[−13]	4.545[−13]	6.117[−13]	7.179[−13]	7.427[−13]	7.379[−13]
1	14	7.167[−14]	1.120[−13]	1.431[−13]	1.538[−13]	1.467[−13]	1.354[−13]
1	15	3.029[−13]	5.255[−13]	7.698[−13]	9.928[−13]	1.092[−12]	1.132[−12]
1	16	4.018[−13]	6.578[−13]	8.978[−13]	1.065[−12]	1.109[−12]	1.105[−12]
1	17	1.197[−13]	1.854[−13]	2.341[−13]	2.480[−13]	2.341[−13]	2.144[−13]
1	18	4.759[−13]	7.703[−13]	1.007[−12]	1.097[−12]	1.051[−12]	9.724[−13]
1	19	4.942[−13]	8.142[−13]	1.089[−12]	1.223[−12]	1.198[−12]	1.127[−12]
1	20	4.791[−13]	7.994[−13]	1.091[−12]	1.275[−12]	1.305[−12]	1.282[−12]
1	21	3.367[−13]	5.611[−13]	7.411[−13]	7.814[−13]	7.087[−13]	6.177[−13]
1	22	2.926[−13]	4.732[−13]	6.165[−13]	6.681[−13]	6.375[−13]	5.874[−13]
1	23	6.000[−13]	9.666[−13]	1.253[−12]	1.351[−12]	1.283[−12]	1.179[−12]
1	24	3.851[−13]	6.216[−13]	8.070[−13]	8.702[−13]	8.271[−13]	7.598[−13]
1	25	1.092[−12]	1.957[−12]	2.907[−12]	3.751[−12]	4.107[−12]	4.238[−12]
1	26	2.972[−13]	4.866[−13]	6.432[−13]	7.096[−13]	6.861[−13]	6.388[−13]
1	27	9.633[−13]	1.702[−12]	2.479[−12]	3.116[−12]	3.349[−12]	3.411[−12]
1	28	2.483[−13]	4.073[−13]	5.364[−13]	5.863[−13]	5.619[−13]	5.192[−13]
1	29	3.308[−13]	5.406[−13]	7.086[−13]	7.703[−13]	7.353[−13]	6.774[−13]
1	30	6.444[−13]	1.168[−12]	1.748[−12]	2.268[−12]	2.488[−12]	2.571[−12]
1	31	2.939[−13]	4.867[−13]	6.462[−13]	7.116[−13]	6.850[−13]	6.349[−13]
1	32	4.261[−13]	7.178[−13]	9.749[−13]	1.106[−12]	1.089[−12]	1.027[−12]
1	33	4.771[−13]	8.317[−13]	1.186[−12]	1.450[−12]	1.528[−12]	1.534[−12]
1	34	2.777[−13]	4.748[−13]	6.380[−13]	6.802[−13]	6.195[−13]	5.411[−13]
1	35	1.416[−11]	2.594[−11]	3.890[−11]	5.016[−11]	5.468[−11]	5.619[−11]
1	36	1.160[−13]	2.008[−13]	2.759[−13]	3.122[−13]	3.047[−13]	2.848[−13]
1	37	1.102[−12]	2.246[−12]	3.779[−12]	5.510[−12]	6.482[−12]	7.011[−12]
1	38	2.107[−13]	3.644[−13]	4.986[−13]	5.605[−13]	5.444[−13]	5.068[−13]
1	39	6.046[−13]	1.064[−12]	1.491[−12]	1.729[−12]	1.718[−12]	1.628[−12]
1	40	6.398[−13]	1.150[−12]	1.605[−12]	1.763[−12]	1.630[−12]	1.436[−12]
1	41	3.518[−13]	6.162[−13]	8.585[−13]	9.905[−13]	9.818[−13]	9.291[−13]
1	42	6.683[−13]	1.184[−12]	1.593[−12]	1.666[−12]	1.491[−12]	1.285[−12]
1	43	4.582[−13]	7.750[−13]	9.892[−13]	9.803[−13]	8.500[−13]	7.173[−13]
1	44	4.668[−13]	8.276[−13]	1.122[−12]	1.191[−12]	1.078[−12]	9.367[−13]
1	45	4.806[−13]	7.541[−13]	9.098[−13]	8.610[−13]	7.280[−13]	6.043[−13]
1	46	5.285[−13]	8.941[−13]	1.141[−12]	1.130[−12]	9.798[−13]	8.268[−13]
1	47	3.844[−13]	5.437[−13]	6.041[−13]	5.587[−13]	4.919[−13]	4.349[−13]
1	48	8.288[−13]	1.588[−12]	2.475[−12]	3.306[−12]	3.678[−12]	3.831[−12]
1	49	7.041[−12]	1.397[−11]	2.265[−11]	3.159[−11]	3.612[−11]	3.832[−11]
1	50	5.879[−13]	1.077[−12]	1.527[−12]	1.697[−12]	1.578[−12]	1.396[−12]
1	51	3.921[−13]	7.074[−13]	9.635[−13]	1.015[−12]	9.101[−13]	7.849[−13]
1	52	3.443[−13]	6.219[−13]	8.471[−13]	8.911[−13]	7.986[−13]	6.882[−13]
1	53	2.800[−13]	5.002[−13]	7.072[−13]	8.251[−13]	8.224[−13]	7.808[−13]
1	54	2.733[−13]	4.942[−13]	6.802[−13]	7.300[−13]	6.647[−13]	5.798[−13]
1	55	6.835[−13]	1.323[−12]	2.071[−12]	2.768[−12]	3.077[−12]	3.201[−12]
1	56	4.588[−13]	6.822[−13]	7.772[−13]	6.934[−13]	5.649[−13]	4.569[−13]
1	57	8.032[−14]	1.439[−13]	2.028[−13]	2.343[−13]	2.312[−13]	2.176[−13]
1	58	4.416[−13]	8.783[−13]	1.414[−12]	1.948[−12]	2.206[−12]	2.325[−12]
1	59	3.581[−11]	7.308[−11]	1.211[−10]	1.719[−10]	1.984[−10]	2.118[−10]

TABLE IV. (*Continued*).

Levels		Electron temperature (eV)					
I	F	500.0	700.0	1000.0	1500.0	2000.0	2500.0
1	60	1.330[−13]	2.460[−13]	3.557[−13]	4.200[−13]	4.196[−13]	3.982[−13]
1	61	7.751[−14]	1.426[−13]	2.052[−13]	2.409[−13]	2.398[−13]	2.270[−13]
1	62	2.721[−13]	5.608[−13]	9.301[−13]	1.314[−12]	1.510[−12]	1.605[−12]
1	63	5.770[−12]	1.174[−11]	1.908[−11]	2.624[−11]	2.956[−11]	3.099[−11]
1	64	1.660[−14]	3.154[−14]	4.659[−14]	5.596[−14]	5.639[−14]	5.379[−14]
1	65	1.312[−13]	2.746[−13]	4.619[−13]	6.623[−13]	7.676[−13]	8.211[−13]
1	66	4.635[−14]	9.098[−14]	1.375[−13]	1.680[−13]	1.706[−13]	1.636[−13]
1	67	2.758[−14]	5.492[−14]	8.409[−14]	1.040[−13]	1.064[−13]	1.025[−13]
1	68	8.906[−14]	1.867[−13]	3.075[−13]	4.237[−13]	4.760[−13]	4.975[−13]
1	69	3.127[−12]	6.732[−12]	1.141[−11]	1.622[−11]	1.859[−11]	1.968[−11]
1	70	2.643[−13]	5.661[−13]	9.548[−13]	1.350[−12]	1.542[−12]	1.630[−12]
1	71	5.329[−14]	1.058[−13]	1.611[−13]	1.977[−13]	2.012[−13]	1.929[−13]
1	72	1.302[−13]	2.587[−13]	3.940[−13]	4.833[−13]	4.915[−13]	4.711[−13]
1	73	7.047[−14]	1.411[−13]	2.168[−13]	2.684[−13]	2.745[−13]	2.643[−13]
1	74	1.437[−12]	3.389[−12]	6.365[−12]	1.011[−11]	1.242[−11]	1.379[−11]
1	75	1.335[−13]	2.874[−13]	4.859[−13]	6.877[−13]	7.852[−13]	8.295[−13]
1	76	6.321[−14]	1.275[−13]	1.967[−13]	2.443[−13]	2.503[−13]	2.411[−13]
1	77	1.760[−13]	3.912[−13]	6.841[−13]	1.004[−12]	1.173[−12]	1.259[−12]
1	78	2.354[−14]	4.936[−14]	7.851[−14]	9.998[−14]	1.039[−13]	1.010[−13]
1	79	1.648[−12]	3.786[−12]	6.746[−12]	9.976[−12]	1.166[−11]	1.251[−11]
1	80	1.312[−13]	2.920[−13]	4.805[−13]	6.009[−13]	5.926[−13]	5.423[−13]
1	81	2.168[−13]	4.766[−13]	8.014[−13]	1.103[−12]	1.226[−12]	1.267[−12]
1	82	1.730[−13]	3.940[−13]	6.921[−13]	1.005[−12]	1.161[−12]	1.235[−12]
1	83	1.975[−13]	4.414[−13]	7.301[−13]	9.180[−13]	9.081[−13]	8.329[−13]
1	84	1.528[−13]	3.370[−13]	5.364[−13]	6.406[−13]	6.128[−13]	5.493[−13]
1	85	1.320[−13]	2.557[−13]	3.647[−13]	3.972[−13]	3.618[−13]	3.145[−13]
1	86	9.386[−14]	2.159[−13]	3.838[−13]	5.654[−13]	6.592[−13]	7.056[−13]
1	87	2.360[−12]	5.692[−12]	1.066[−11]	1.659[−11]	2.002[−11]	2.194[−11]
1	88	3.749[−13]	9.681[−13]	1.954[−12]	3.295[−12]	4.174[−12]	4.721[−12]
1	89	4.410[−14]	9.541[−14]	1.551[−13]	2.007[−13]	2.098[−13]	2.046[−13]
1	90	5.365[−14]	1.178[−13]	1.943[−13]	2.549[−13]	2.691[−13]	2.642[−13]
1	91	1.163[−13]	2.713[−13]	4.865[−13]	7.191[−13]	8.383[−13]	8.964[−13]
1	92	7.193[−15]	1.666[−14]	2.840[−14]	3.664[−14]	3.674[−14]	3.397[−14]
1	93	1.960[−14]	4.666[−14]	8.585[−14]	1.312[−13]	1.566[−13]	1.704[−13]
1	94	2.890[−14]	6.871[−14]	1.190[−13]	1.550[−13]	1.559[−13]	1.443[−13]
1	95	7.161[−14]	1.885[−13]	3.849[−13]	6.545[−13]	8.328[−13]	9.448[−13]
1	96	6.683[−14]	1.641[−13]	2.911[−13]	3.857[−13]	3.912[−13]	3.639[−13]
1	97	1.288[−13]	3.119[−13]	5.322[−13]	6.698[−13]	6.570[−13]	5.974[−13]
1	98	8.852[−14]	2.197[−13]	4.113[−13]	6.268[−13]	7.409[−13]	7.985[−13]
1	99	8.826[−13]	2.308[−12]	4.588[−12]	7.479[−12]	9.234[−12]	1.025[−11]
1	100	2.103[−14]	4.713[−14]	7.968[−14]	1.039[−13]	1.053[−13]	9.821[−14]
1	101	6.346[−14]	1.684[−13]	3.367[−13]	5.493[−13]	6.773[−13]	7.511[−13]
1	102	3.185[−14]	7.713[−14]	1.366[−13]	1.892[−13]	2.049[−13]	2.043[−13]
1	103	1.406[−13]	3.825[−13]	7.851[−13]	1.316[−12]	1.648[−12]	1.848[−12]
1	104	4.632[−14]	1.261[−13]	2.360[−13]	3.204[−13]	3.268[−13]	3.042[−13]
1	105	6.493[−14]	1.730[−13]	3.338[−13]	5.017[−13]	5.716[−13]	5.902[−13]
1	106	8.280[−14]	2.257[−13]	4.221[−13]	5.719[−13]	5.824[−13]	5.417[−13]
1	107	2.920[−13]	8.461[−13]	1.811[−12]	3.117[−12]	3.948[−12]	4.450[−12]

cm^2, 63 ($3p_{3/2}$-$4p_{3/2}$) with a cross section of 2.3×10^{-20} cm^2, and 69 ($3p_{1/2}$-$4p_{1/2}$) with a cross section of 1.4×10^{-20} cm^2. One might expect the $3s$-$4s$ "monopole" ($E0$) transition (1-79) to be smaller (0.9×10^{-20} cm^2) as there are only two $3s$ electrons, which are buried deeply in the M shell. On the other hand, the monopole transition involving $3d_{5/2}$ electrons might be expected to be quite large, as there are initially six $3d_{5/2}$ electrons, and they

are not at all deeply buried. The present results for the near-threshold excitation cross section is a small 0.3×10^{-20} cm^{-2}, which seems to be smaller than might otherwise be expected. A possible explanation may be that the two $J = 0$ $4d$ states separate themselves in Gd in nearly LS coupling, and that state 35 ($3s^2 3p_{1/2}^2 3p_{3/2}^4 3d_{3/2}^3 3d_{5/2}^6 4d_{3/2}$) is the excited $4d$ $^1S_0$ state. In such a picture, the dominant collisional excita-

tion would be to level 35 by monopole excitation, and excitation to level 27 would be made up of exchange contribution plus a minor amount of direct excitation from mixing with the $^1S_0$.

The strong monopole excitation cross sections to states 35, 63, and 69 are very interesting, as these states might make good candidates for upper laser states in possible soft-x-ray laser experiments based on electron collisional excitation.[2]

The only other transition which exceeds 10^{-20} cm^2 near threshold is a $3p_{3/2}$-$4f_{7/2}$ transition to level 87, which is a $J=2$ state. This transition is the strongest electric quadrupole ($E2$) transition, with a near-threshold cross section of 1.2×10^{-20} cm^2.

[1]S. Maxon, P. Hagelstein, K. Reed, and J. Scofield, J. Appl. Phys. **57**, 971 (1985).

[2]S. Maxon, P. Hagelstein, J. Scofield, and Y. Lee, J. Appl. Phys. **59**, 239 (1986).

[3]A. G. Molchanov, Usp. Fiz. Nauk **106**, 165 (1972) [Sov. Phys.—Usp. **15**, 124 (1972)].

[4]M. A. Duguay, Laser Focus **9**, 41 (1973).

[5]R. C. Elton, Appl. Opt. **14**, 97 (1975).

[6]K. G. Whitney and J. Davis, J. Appl. Phys. **46**, 4103 (1975).

[7]A. N. Zherikhin, K. N. Koshelev, V. S. Letokhov, Kvant. Elektron. (Moscow) **3**, 152 (1976) [Sov. J. Quantum Electron. **6**, 82 (1976)].

[8]L. J. Palumbo and R. C. Elton, J. Opt. Soc. Am. **67**, 480 (1977).

[9]K. G. Whitney, J. Davis, and J. P. Apruzese, *Cooperative Effects in Matter and Radiation,* edited by Bowen et al. (Plenum, New York, 1977), p. 115.

[10]A. Ilyukhin, G. V. Peregudov, E. N. Ragozin, I. I. Sobel'man, and V. A. Chirkov, Pis'ma Zh. Eksp. Teor. Fiz. **25**, 569 (1977) [JETP Lett. **25**, 536 (1977)].

[11]L. A. Vainshtein, A. V. Vinogradov, U. I. Safronova, and I. Yu. Skobelev, Kvant. Elektron. (Moscow) **5**, 417 (1978) [Sov. J. Quantum Electron. **8**, 239 (1978)].

[12]U. Feldman, A. K. Bhatia, and S. Suckewer, J. Appl. Phys. **54**, 2188 (1983).

[13]J. P. Apruzese and J. Davis, Phys. Rev. A **28**, 3686 (1983).

[14]A. V. Vinogradov and V. N. Shlyaptsev, Kvant. Elektron. (Moscow) **10**, 516 (1983) [Sov. J. Quantum Electron. **13**, 303 (1983)].

[15]U. Feldman, J. F. Seely, and A. K. Bhatia, J. Appl. Phys. **56**, 2475 (1984).

[16]M. D. Rosen, P. L. Hagelstein, D. L. Matthews, E. M. Campbell, A. U. Hazi, B. L. Whitten, B. MacGowan, R. E. Turner, R. W. Lee, G. Charatis, Gar. E. Busch, C. L. Shepard, P. D. Rockett, and R. R. Johnson, Phys. Rev. Lett. **54**, 106 (1985).

[17]D. L. Matthews, P. L. Hagelstein, M. D. Rosen, M. J. Eckart, N. M. Ceglio, A. U. Hazi, H. Medecki, B. J. MacGowan, J. E. Trebes, B. L. Whitten, E. M. Campbell, C. W. Hatcher, A. M. Hawryluk, R. L. Kauffman, L. D. Pleasance, G. Rambach, J. H. Scofield, G. Stone, and T. A. Weaver, Phys. Rev. Lett. **54**, 110 (1985).

[18]W. Eissner and M. J. Seaton, J. Phys. B **5**, 2187 (1972); H. E. Saraph, Comput. Phys. Commun. **1**, 232 (1970); M. A. Crees, M. J. Seaton, and P. M. H. Wilson, Comput. Phys. Commun. **15**, 23 (1978); M. Klapisch (private communication).

[19]D. W. Walker, J. Phys. B **2**, 356 (1969).

[20]G. D. Carse, and D. W. Walker, J. Phys. B **6**, 2529 (1973).

[21]D. W. Walker, J. Phys. B **2**, 356 (1969).

[22]D. W. Walker, J. Phys. B **7**, 97 (1974).

[23]J. Chang, Phys. Rev. A **12**, 791 (1975).

[24]J. J. Chang, J. Phys. B **10**, 3335 (1977).

[25]P. H. Norrington and I. P. Grant, J. Phys. B **14**, L261 (1981).

[26]I. P. Grant, Comput. Phys. Commun. **5**, 263 (1973).

[27]I. P. Grant and N. C. Pyper, J. Phys. B **9**, 761 (1976).

[28]I. P. Grant, B. J. McKenzie, and P. H. Norrington, Comput. Phys. Commun. **21**, 207 (1980).

[29]P. L. Hagelstein and R. K. Jung, Lawrence Livermore Laboratory Report UCRL-93588, 1985, unpublished.

[30]P. L. Hagelstein, Phys. Rev. A **34**, 924 (1986), this issue.

[31]P. L. Hagelstein and R. K. Jung, presented at the Third International Conference/Workshop on the Radiative Properties of Hot Dense Matter, Williamsburg, 1985 (unpublished).

[32]J. H. Scofield (unpublished). The RAC code has been used at LLNL for nearly a decade for a wide variety of energy-level and oscillator-strength calculations.

[33]I. P. Grant, Adv. Phys. **19**, 747 (1970).

[34]P. G. Burke, Comput. Phys. Commun. **1**, 241 (1970).

[35]P. J. Mohr, Ann. Phys. (NY) **88**, 52 (1974); Phys. Rev. Lett. **34**, 1050; Phys. Rev. A **26**, 2338.

[36]E. A. Uehling, Phys. Rev. **48**, 55 (1935); G. Soff and B. Muller, Z. Naturforsch. **29**, 1267 (1974).

[37]M. H. Chen, B. Crasemann, M. Aoyagi, K. Huang, and H. Mark, At. Data Nucl. Data Tables **26**, 561 (1981).

[38]G. D. Pollak (unpublished). The code is called PSEUDO, and allows the inclusion of pseudo-state orbitals generated heuristically to be included in the relativistic CI expansion. This code has been incorporated into the YODA package of Ref. 30.

[39]J. P. Desclaux, D. F. Mayers, and F. O. O'Brien, J. Phys. B At. Mol. Phys. **4**, 631 (1971).

[40]G. D. Pollak (unpublished).

[41]M. J. Seaton, Proc. Phys. Soc. London **77**, 174 (1960).

[42]M. J. Seaton, Philos. Trans. R. Soc. London **245**, 469 (1953); H. E. Saraph, M. J. Seaton, and J. Shemming, *ibid.* **264**, 77 (1969); P. G. Burke, and K. E. Smith, Rev. Mod. Phys. **34**, 458 (1962); K. Smith, R. J. W. Henry, and P. G. Burke, Phys. Rev. **147**, 21 (1966).

[43]P. G. Burkhalter, D. J. Nagel, and R. R. Whitlock, Phys. Rev. A **9**, 2331 (1974); P. G. Burkhalter, C. M. Dozier, and D. J. Nagel, *ibid.* **15**, 700 (1977).

[44]A. Zigler, H. Zmora, N. Spector, M. Klapisch, J. L. Schwob, and A. Bar-Shalom, J. Opt. Soc. Am. **70**, 129 (1980).